Conf-730705--12

LA-UR - 73 - 1053

TITLE: REVIEW OF SCYLLAC THETA-PINCH EXPERIMENTS

AUTHOR(S): W. E. QUINN, W. R. ELLIS, R. F. GRIBBLE, C. R. HARDER, R. KRISTAL, F. L. RIBE, G. A. SAWYER, R. E. SIEMON AND K. S. THOMAS

SUBMITTED TO: TO BE PRESENTED AT SIXTH EUROPEAN CONFERENCE ON PLASMA PHYSICS AND CONTROLLED NUCLEAR FUSION RESEARCH, MOSCOW, U.S.S.R., JULY 30 - AUGUST 3, 1973.

los alamos scientific laboratory
of the University of California
LOS ALAMOS, NEW MEXICO 87544

rm No. 836
. No. 2629
73

UNITED STATES
ATOMIC ENERGY COMMISSION
CONTRACT W-7405-ENG. 36

REVIEW OF SCYLLAC THETA-PINCH EXPERIMENTS*

by

W. E. Quinn, W. R. Ellis, R. F. Gribble, C. R. Harder, R. Kristal, F. L. Ribe, G. A. Sawyer, R. E. Siemon and K. S. Thomas

Los Alamos Scientific Laboratory, University of California, Los Alamos, New Mexico U. S. A.

ABSTRACT:

Scyllac research on 5-m and 8-m toroidal sectors, and the 5-meter linear theta-pinch are discussed. In addition, we outline the plans for the full Scyllac torus, feedback stabilization, and a staged theta-pinch.

I. INTRODUCTION

Linear θ-pinch experiments during the past decade and a half have demonstrated the production of hot, dense, stable plasmas. The limitation on the time of confinement of these plasmas has been end loss and not escape across the magnetic field by means of macro- or micro-instabilities. In view of the end-loss containment limitation in linear systems the large aspect ratio toroidal θ-pinch Scyllac is being constructed at Los Alamos. During the past two years "Scyllac" research has been divided among four major experimental efforts: 1) 5-meter[1,2] and 8-meter, 120° toroidal sectors; 2) a 5-meter linear theta pinch with strong magnetic mirrors[2,3]; 3) studies of the $\ell = 1,0$ interference force and the MHD $m = 1$ instability with $\ell = 1$ and $\ell = 0$ fields on the 3-meter linear Scylla IV device[4]; and 4) the development of a feedback system for stabilizing the $m = 1$ instability[5]. The objective of these experiments, other than the linear Scyllac, has been to study various aspects of the equilibrium and stability of the high-β θ-pinch in toroidal geometry.

In the Scyllac sector, with a major radius R and plasma radius a, the toroidal drift force $F_R = \beta B_o^2 a^2/4R$ is compensated by a combination of $\ell = 1$ helical and $\ell = 0$ bumpy fields. The toroidal equilibrium [6,7,8] of this system and the stability [8,9,10,11] of a straight $\ell = 1$ or $\ell = 0$ plasma column have been treated in the MHD approximation. The $\ell = 1$ field is chosen because: 1) theory predicts a growth rate for the dominant $k \approx 0$, $m = 1$ mode which vanishes in leading order; and 2) in high β, high temperature theta pinches [5] only long wavelength, $m = 1$ modes are observed experimentally. The $\ell = 0$ fields produce the asymmetry in the sum of the plasma excursions $\delta_1 \approx B_{\ell=1}/B_o\, ha(1-\beta/2)$ and $\delta_o \approx -B_{\ell=0}/2B_o(1-\beta)$ which is needed t. produce the equilibrating force, $F_{1,0} = \beta(3-2\beta)\, B_o^2h^2a^3\delta_1\delta_o/8$, where $2\pi/h$ is the wavelength of the $\ell = 1,0$ fields. Equating the outward toroidal force to the $F_{1,0}$ force gives the equilibrium condition $\delta_1\delta_o \approx 2/(3-2\beta)h^2aR$. In the initial toroidal-sector experiments [1,2,] with the $\ell = 1$ helical field provided by capacitor-driven windings and the $\ell = 0$ field formed by rectangular grooves in the inner surface of the compression coil, the plasma was observed to take up a helical toroidal equilibrium for 4 to 8 μsec in contrast to the case with no $\ell = 1$ field where the plasma accelerated immediately to the outer wall of the torus. Following the equilibrium period an $m = 1$, $k \approx 0$ sideward motion of the plasma column carried the plasma to the wall. Thus the plasma confinement is terminated in 6 to 10 μsec by $m = 1, k = 0$ transverse motion, whose characteristics were not differentiated between instability and loss of equilibrium. These experiments verified the theoretical MHD equilibrium of the toroidal Scyllac sector.

The experiments on both the 5-m toroidal sector (R = 2.4 m) and the 5-m linear Scyllac have been completed. The Scyllac system is now being converted to its full toroidal configuration. Results on the sector and on the Scylla IV-3 feedback experiment indicated the necessity of increasing the Scyllac major diameter from 4.8 to 8.0 m to decrease the growth rate of the $m = 1$, $k = 0$ instability to accommodate the technical characteristics of the feedback apparatus (cf. Sec. III below). The conversion of one-third of the torus to the larger radius has been completed and experiments resumed in this sector with an 8.4-m coil to study the plasma equilibrium and stability in the larger radius of curvature, prior to experiments on the full torus.

In present θ-pinches, the plasmas occupy only a small fraction of the coil radius. Because of this it is anticipated that the $m = 1$ MHD instability driven by the helical fields which produce toroidal equilibrium in Scyllac-type experiments must be feedback stabilized. Theoretical studies indicate that with larger plasma radii (more implosion heating, less compression heating) the feedback can be dispensed with in favor of stabilization by the conducting wall as in the staged θ pinch [12].

Experiments are beginning at LASL to study implosion heating and staging in theta pinches. Previous theta pinches have performed initial implosion heating of the ions and subsequent adiabatic compression with a single capacitor bank power supply. Projected theta-pinch feasibility experiments and fusion reactors will require separation of the two functions to achieve greater implosion heating and less adiabatic compression. One experiment will study the implosion-heating processes, and, a second will combine implosion heating with separate adiabatic compression (staging).

The objectives of the 5-m linear Scyllac were to study the effects of strong magnetic mirrors on the confinement and stability of a high β plasma and to provide scaling data on end loss and electron temperature with plasma length. Results of experiments both with and without magnetic mirrors are reported.

II. EXPERIMENTS WITH ℓ = 1,0 HELICAL EQUILIBRIA IN THE 5-m AND 8-m TOROIDAL SECTORS

A. Experimental Arrangement.

For the past two years, Scyllac has been assembled in a preliminary configuration as a 5-meter long toroidal sector and a separate 5-meter linear theta pinch with strong mirrors as shown in the plan view of Fig. 1. The initial Scyllac toroidal sector [1,2] had a major radius of 237.5 cm, extended through an angle of 120° and had a coil arc length of 5 m. Each meter section of the compression coil was driven by a 700-kJ capacitor bank of 210 1.85-μF, 60 kV capacitors. The experiments were performed with one-half the bank charged to 45 and 50 kV to produce peak magnetic compression fields of 33 to 50 kG with risetimes of ~ 4 μsec, followed by crowbarred waveforms with L/R times of 250 μsec. The compression coil inner diameters were in the range of 14.4 to 20.5 cm and the inside diameter of the quartz discharge tube was 8.8 cm. A 50 kV, 0.9-kJ/m, θ-preionization bank, which produces a 400 kHz oscillating field, was used to preionize the initial deuterium gas fillings of 10 to 20 mTorr. In the initial experiments the ℓ = 1 fields were applied by means of capacitor driven, bifilar helical windings and the ℓ = 0 fields were generated by annular grooves in the inner surface of the compression coil.

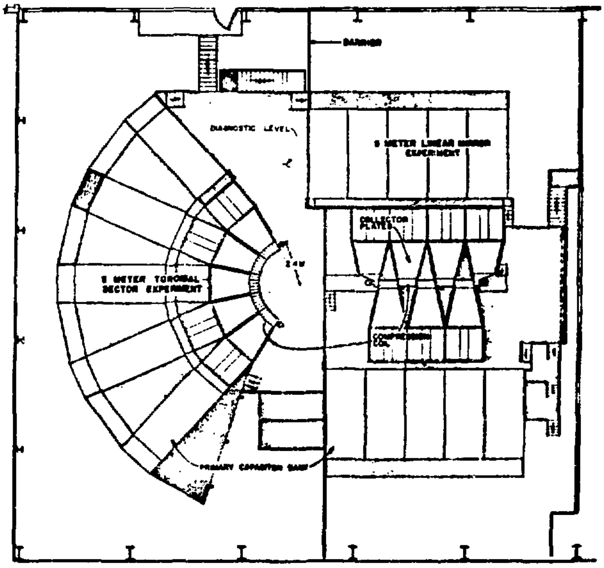

Fig. 1. Plan view showing arrangement of Scyllac 5-m toroidal sector and 5-m linear theta pinch.

A second set of experiments was performed in shaped compression coils in which the flux surfaces of the ℓ = 1 and ℓ = 0 fields were machined into the inner surface of the main coils. The advantages of this ℓ = 1,0 configuration are: (1) a constant ratio of both the ℓ = 1 and ℓ = 0 fields to the main field in time; (2) an improvement in the uniformity of the ℓ = 1 and ℓ = 0 fields; and (3) a technical simplification of the generation of the ℓ = 1 and ℓ = 0 fields. A disadvantage of this geometry is the fixed ratios of the ℓ = 1 and ℓ = 0 fields to the main toroidal field, B_0.

The new sector, which comprises one-third of the final Scyllac torus, has a larger major radius of 4.0 meters and a coil arc length of 8.4 meters; the ℓ = 1,0 equilibrium fields are generated by the shaped inner surface of the compression coil. The design product of these fields was determined through the sharp-boundary equilibrium relations [8] to give $B_{\ell=1} B_{\ell=0}/B_o^2 = f(\beta, ha)\, ha^2/R$. A graph of the equilibrium field-product ratio, $B_{\ell=1} B_{\ell=0}/B_o^2$, for β in the range of 0.6 to 0.9 is given in Fig. 2 for plasma radii in the range of 0.6 to 1.0 cm. Equal magnitudes of $B_{\ell=1}$ and $B_{\ell=0}$ were chosen; this produces a bumpiness δ_o of the plasma column which is small compared with the helical displacements δ_1. The experimental points on Fig. 2 show the agreement of the observed toroidal equilibrium with sharp boundary theory in the 5-m sector. (Measured radii = 0.7-0.8 cm).

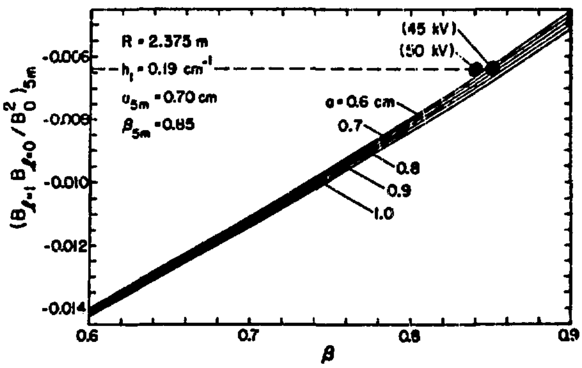

Fig. 2. Values of $B_{\ell=1} B_{\ell=0}/B_o^2$ predicted by sharp boundary theory for plasma equilibrium in the 5-m toroidal sector. Experimental points $(B_{\ell=1} B_{\ell=0}/B_o^2 = -0.0064$; $\beta = 0.85$, $a = 0.7$ cm; $\beta = 0.8$, $a = 0.8$ cm) are shown for 45 and 50 kV bank voltages.

The designs of the shaped coils were determined by calculating the shape of the magnetic flux surfaces for the required vacuum fields from

$$\overline{B}/B_o = \hat{e}_z \left(1 - \frac{r}{R}\cos\theta\right) + \nabla\phi\,, \qquad (1)$$

where

$$\phi = (B_{\ell=1}/B_o)\,[2\, I_1(hr)/h]\sin(\theta - hz) + (B_{\ell=0}/B_o)[I_o(hr)/h]\sin hz + (B_v/B_o)\, r\sin\theta + (B_{1,2}/B_o)\sin(\theta - 2hz). \qquad (2)$$

The small vertical field B_v and $B_{1,2}$ field are required for equilibrium according to the sharp boundary theory. The amplitudes of these fields are given by

$$\frac{B_v}{B_o} = \frac{B_{1,2}}{B_o} = \frac{B_{\ell=1}B_{\ell=0}}{4B_o^2}\,. \qquad (3)$$

The $B_{1,2}$ field varies in space as $\sin(\theta - 2hz)$, and produces a small ellipticity in the plasma cross section, in contrast to the $\ell = 1$ field with $\sin(\theta - hz)$. Each wavelength, $\lambda_{1,0} = 41.9$ cm, of the 8-m sector was divided into 330 steps with 1.25 mm/step and flux surfaces calculated for each step. A vertical field amplitude of $B_v/B_o = 0.00168$, 44% larger than the theoretical value, was used to give flux surfaces at the coil wall which have circular cross sections for simplicity of machining. This larger value of vertical field shifts the inner flux surfaces inward in the horizontal plane and decreases their area. With this design the vacuum flux surfaces can be centered in the discharge tube by the addition of a vertical field from driven windings.

B. Results.

During the past year an extensive series of experiments on the Scyllac 5-m toroidal sector was completed. These included nine variations of $\ell = 0$ and $\ell = 1$ magnetic fields to provide toroidal equilibrium against the drift force F_R. The value of the $\ell = 1,0$ equilibrium fields in the 8-m sector experiment was scaled from the 5-m results. In both the 5-m and 8-m experiments with deuterium filling pressures of 10 to 20 mTorr, the average plasma β on axis is 0.7 to 0.9, the ion temperature 0.8 to 1.0 keV, and the plasma density 2 to 3 x $10^{16} cm^{-3}$.

The following measurements were made of the plasma properties: (1) three high-speed streak cameras, viewing the plasma column side-on were used to record the transverse motions of the plasma column; (2) a coupled-cavity He-Ne laser interferometer was used to measure the time history of plasma electron density integrated along a chord of the plasma cross section; (3) a magnetic loop and probe arrangement was used to measure the magnetic flux excluded by the plasma. Combined with density profiles from the luminosity, the excluded flux can be expressed in terms of the plasma β; (4) a ten-channel, side-on luminosity experiment was used to obtain the intensity profiles of the plasma column. These luminosity profiles, in conjunction with the coupled-cavity interferometer data, give absolute density profiles; and (5) scintillation and silver-foil activation counters were used to measure the neutron emission.

1. Plasma Equilibrium and Stability. The streak photographs of Fig. 3A show the horizontal plasma motions in the 5-meter toroidal sector in the absence of $\ell = 1$ fields. The motion is a simple toroidal "drift" to the walls with no observable effect induced by the presence of bumpy $\ell = 0$ fields. In Fig. 3B the $\ell = 1$ coils were excited to 56 kA. After remaining in equilibrium for 6 μsec, the plasma begins to drift outward in both the land and groove regions and strikes the wall in the land region. The experiments show the following: (1) the plasma column takes up an initial helical shift and comes into an equilibrium position which lasts 4 to 8 μsec, in contrast to a complete absence of equilibrium without the $\ell = 1,0$ fields; (2) as the plasma moves away from the equilibrium position, the motion in the land and groove regions is usually similar, i.e., the column either moves radially outward or inward; (3) the motion of the plasma column develops largely in the horizontal plane of the torus rather than in random directions; and

(4) a few percent increase (or decrease) in the $\ell = 1$ equilibrium field causes the plasma column to move radially inward (or outward) away from its equilibrium position in both land and groove regions.

In experiments on both the 5-m and 8-m sectors with fixed $\ell = 1$ and $\ell = 0$ fields generated by the $\ell = 1,0$ shaped inner surface of the toroidal coils, the plasma equilibrium was achieved by adjusting the initial deuterium filling pressure to give a balance between the $F_{1,0}$ and toroidal F_R forces through their β dependence. The equilibrium and stability of the high-β plasma produced in the shaped $\ell = 1,0$ coils have been studied in the toroidal sector both with and without additional applied vertical fields (B_V = 100 to 600 G). The plasma confinement is slightly improved when the vertical field windings are excited to produce the theoretical vertical field amplitude of Eq. (3), but is not critically dependent on the magnitude of the vertical field. This result indicates that flux surfaces are not important in the sector experiments since larger values of the vertical field shift the vacuum flux surfaces at least partially out of the discharge tube cross section. However, flux surfaces are likely to be important on the longer time scale of the full torus.

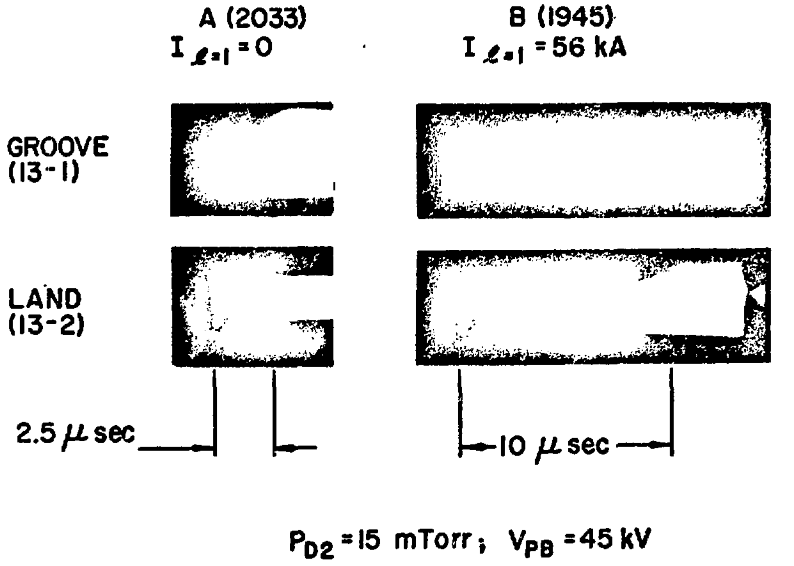

Fig. 3. Streak photographs of the 5-m toroidal sector plasma showing horizontal motion with and without $\ell = 1$ fields.

The streak photographs of Fig. 4 compare the plasma transverse motions in the 5-m and 8-m sectors with shaped compression coils. The general characteristics of the plasma motions are similar to those observed with the $\ell = 1$ driven windings, except that the long wavelength m = 1 motion tends to be somewhat more random in direction. As in the experiments with driven $\ell = 1$ windings, where a small change in the magnitude of the $\ell = 1$ fields moved the plasma from its equilibrium position, in the shaped coils with fixed $\ell = 1,0$ field ratios a few percent change in the deuterium filling pressure, with a corresponding change in plasma β, produces the same results.

The examination of many streak photographs shows that the plasma column remains in stable equilibrium for 7 to 10 μsec in the 8-m sector, compared with 4 to 7 μsec in the 5-m experiment, at which times the onset of the terminating m = 1 sideward motion occurs. The ratio of the onset times, $\tau_{os}(8m)/\tau_{os}(5m) \simeq 1.5$ can be compared with the Alfvén times, $\tau_A(8m)/\tau_A(5m) \simeq 1.6$, from the ends of the sectors to the center, and with the plasma end-loss times, $\tau_p(8m)/\tau_p(5m) \simeq 1.7$. Thus, the onset-time scaling is in good agreement with the assumption that it is produced by end-effects. The plasma is apparently stable until end effects propagate to the center of the sector. Assuming that the motion which terminates the stable period is the instability predicted by the theory, its measured growth rates are $\gamma_1(5m) \simeq 1.1$ MHz and $\gamma_1(8m) \simeq 0.6$ MHz. Theory [8] gives the following dispersion relation for the m = 1 mode:

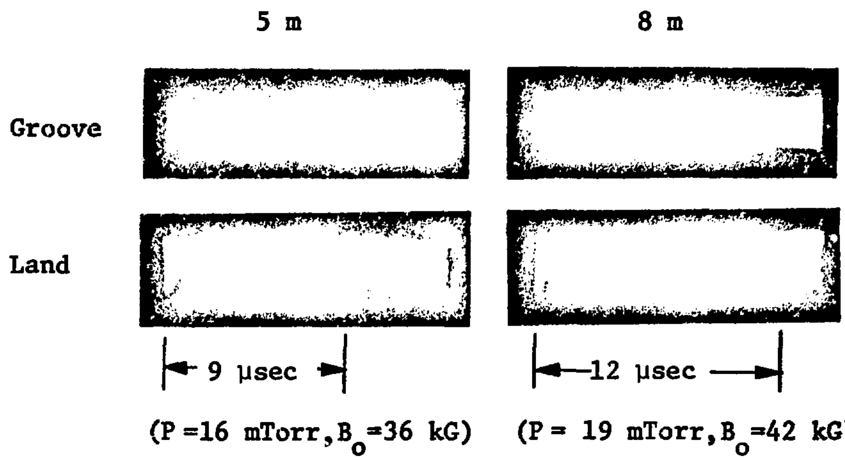

Fig. 4. Streak photographs comparing plasma behavior in the 5-m and 8-m toroidal sector experiments.

$$\gamma_1^2 = h^2 v_A^2 \delta_1^2 \left[-\beta^2 \left(\frac{a}{b}\right)^4 + \frac{\beta(4-3\beta)(2-\beta)}{8(1-\beta)} h^2 a^2 \right] \simeq \frac{\beta(4-3\beta)}{2(1-\beta)(2-\beta)} v_A^2 h^2 \left(\frac{B_{\ell=1}}{B_o}\right)^2, \quad (4)$$

where the a/b term arises from wall stabilization and is small in the present experiments. The calculated growth rates are 1.0 MHz and 0.6 MHz for the 5-m and 8-m experiments,respectively. Thus the terminating γ_1's scale between the 5-m and 8-m experiments in good agreement with the theory. The scaling of the equilibrium -field product $(B_{\ell=1} B_{\ell=0}/B_o^2 = f(\beta, ha)\, ha^2/R)$ from the 5-m to the 8-m experiment, given by sharp-boundary theory,has also been confirmed by experiment. This is shown in Fig. 5 where the curves represent the 8-m equilibrium field ratio scaled theoretically from its value at 5 meters (Fig. 2). The measured 8-meter ratio is shown by the horizontal dashed line, and the two points give the limits of the measured values of β.

2. <u>Measurements of Plasma Parameters.</u> Measurements have been made of the plasma radius as a function of time, determined by side-on luminosity profiles, and plasma excluded flux, determined by the balanced probe method. These data

have been combined to yield the plasma beta as a function of time. These variables have been measured in positions of minimum and maximum plasma radius [land (L) and groove (G), respectively] in order to study the approach of the plasma column to theoretically predicted transverse (or toroidal) and axial equilibrium.

According to sharp boundary (SB) theory, there exists for each plasma radius a unique value of beta for which toroidal equilibrium is possible. Figure 6 compares this predicted value of beta in a land for experiments J(5m) and K(8m) (using the observed plasma radius) with the measured plasma beta on axis. Theory and experiment show excellent agreement at later times, confirming the streak photograph behavior (cf. Fig. 4), but not at earlier times when axial pressure equilibrium between lands and grooves has not yet been achieved.

A basic assumption of the SB theory is axial pressure equilibrium, i.e. nkT = constant independent of length, which requires $\beta_L/\beta_G = (B_G/B_L)^2$. This test has been applied to these data to study the approach to axial equilibrium, as shown in Fig. 7. The measured magnetic field ratio is compared to the design ratio $(B_G/B_L)^2 = (1 - B_{\ell=0}/B_o)^2/(1 + B_{\ell=0}/B_o)^2$, and also to the measured value of β_L/β_G as a function of time.

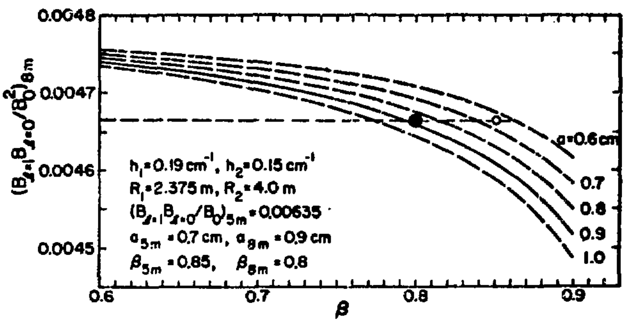

Fig. 5. Values of $B_{\ell=1}\, B_{\ell=0}/B_o^{\,2}$ predicted for plasma equilibrium in the toroidal sector, scaled from the 5-m-sector equilibrium. Experimental points are shown

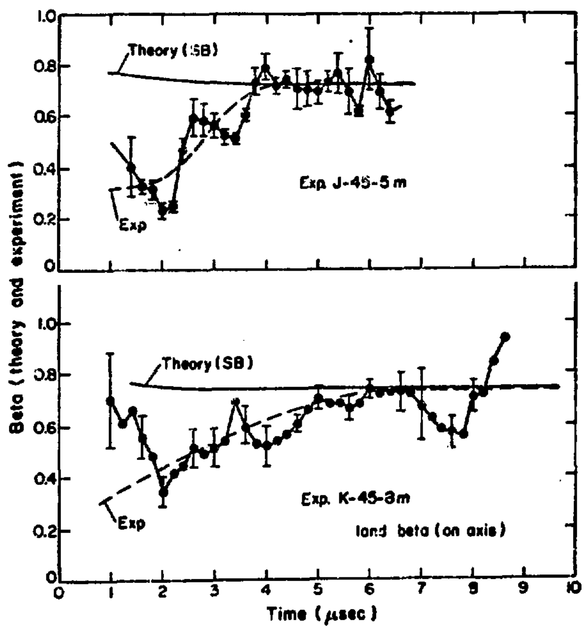

Fig. 6. Comparison of predicted and measured beta on axis vs. time in a land region from the 5-m (top) and 8-m (bottom) toroidal sector experiments.

The plasma is seen to reach axial equilibrium in ∿ 4 μsec in Exp. J (wavelength =

33 cm) and ~ 6 μsec in Exp. K (wavelength = 42 cm), and the β variation with time is consistent with a transfer of energy density from grooves to lands during this period.

Measurements of the plasma radius, beta, and magnetic field in the various experiments thus confirms in detail the stable toroidal equilibrium seen in the streak photographs during the first 4-10 μsec of the discharge. The initial absence of axial pressure equilibrium does not appear to affect the experimental toroidal force balance.

III. FEEDBACK STABILIZATION SYSTEM FOR THE SCYLLAC TORUS

A. Feedback Considerations.

An $\ell = 0$ MHD feedback stabilization system has been developed for Scyllac to control the long wavelength $m = 1$ motion. The feedback control is implemented through the generation of small controllable $\ell = 0$ fields which interfere with the $\ell = 1$ equilibrium field to produce a perturbation $F_{1,0}$ feedback force. This is the same type of transverse body force that provides the toroidal equilibrium in the curved geometry and has been previously shown to exert the predicted force on a deliberately induced $m = 1$ instability in the linear Scylla IV-3 experiment [4]. Its magnitude per unit length is given by sharp-boundary theory as $F_{1,0} = [\beta(3-2\beta)/8]\ B_o^2\ h^2 a^3 \delta_1 \delta_o$ where δ_o is the plasma bumpiness produced by the $\ell = 0$ feedback fields. The destabilizing force per unit length due to the $\ell = 1$ fields is $F_1 = \pi a^2 \rho \gamma_1^2 \xi$, where ρ is the plasma mass density on axis, and ξ is the displacement from equilibrium. Equating these two forces and utilizing the approximate relations for δ_o and δ_1 gives the required feedback current to each $\ell = 0$ coil:

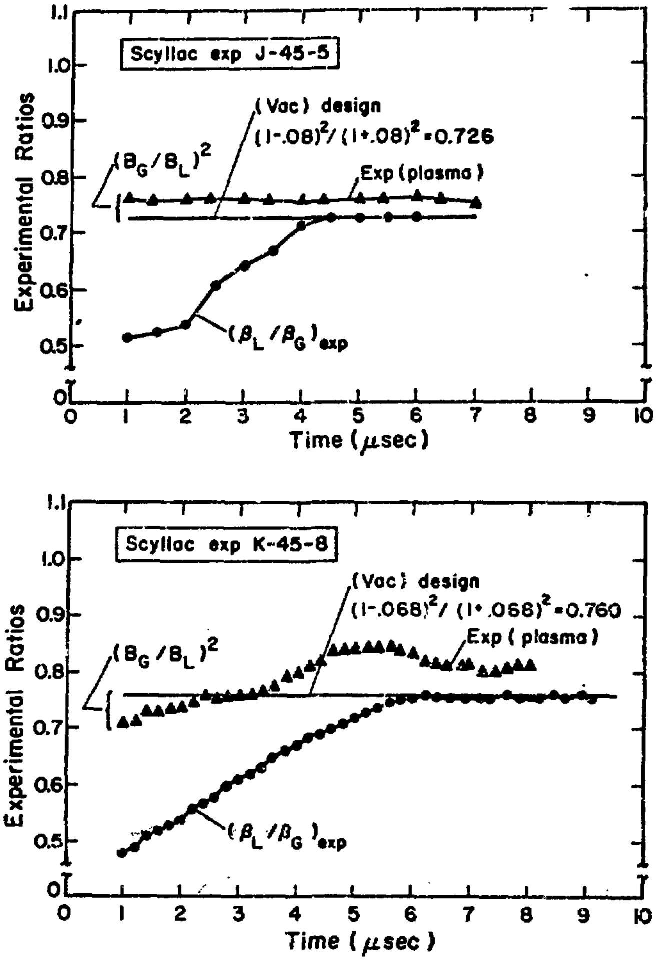

Fig. 7. Comparison of the measured ratio of beta's in the land and groove regions with experimental and design ratios of the magnetic field corresponding to axial pressure equilibrium. The upper curves are for the 5-m and the lower curves for the 8-m experiment.

$$I_{FB} = \frac{80(1-\beta)(1-\beta/2)}{\beta(3-2\beta)} \frac{\rho\gamma_1^2\xi}{B_o h B_{\ell=1}/B_o} = 5 \frac{(4-3\beta)}{(3-2\beta)} f B_o \xi \frac{B_{\ell=1}}{B_o} \propto (hR)^{-1/2}, \qquad (5)$$

where $\delta_o = hI_{FB}/10(1-\beta) B_o f$ and f is a geometrical parameter of the $\ell = 0$ feedback coil. Computer modeling [14] indicates the additional constraint that the electrical system delay τ be less than $1/\gamma_1$.

B. Experimental Arrangement of the Feedback Stabilization System.

In Scyllac both the $\ell = 1$ and $\ell = 0$ equilibrium fields are generated by the shaped inner surface of the main compression coil, while the $\ell = 0$ feedback fields are generated by single-turn slotted coils inside the main coil as illustrated in Fig. 8. The feedback stabilization system consists of many components, starting with plasma-position optical detectors, and ending with power amplifier modules which drive the $\ell = 0$ coils.

Experience with the feedback equipment has been gained on the 3-m Scylla IV device, with 10 modules installed to provide a feedback force in one coordinate. These modules were used in a test of their ability to handle an instability that was deliberately induced with $\ell = 1$ fields. With $B_{\ell=1}/B_o = 0.04$, an m = 1 instability growth rate of 0.9 MHz was observed. The feedback system produced a 160 G field in the $\ell = 0$ coils, and with delayed turn-on times as great as 0.5 μsec following the initiation of the discharge, the module output was successful in overcoming the plasma motion to the wall. In Scyllac the feedback system will have a capability of 4.0 kA ($B_{\ell=0}$ = 235 G) with a risetime of 0.9 μsec. With the theoretically predicted growth rate in Scyllac of 0.6 MHz, the feedback should be able to control a plasma displacement of 6 mm.

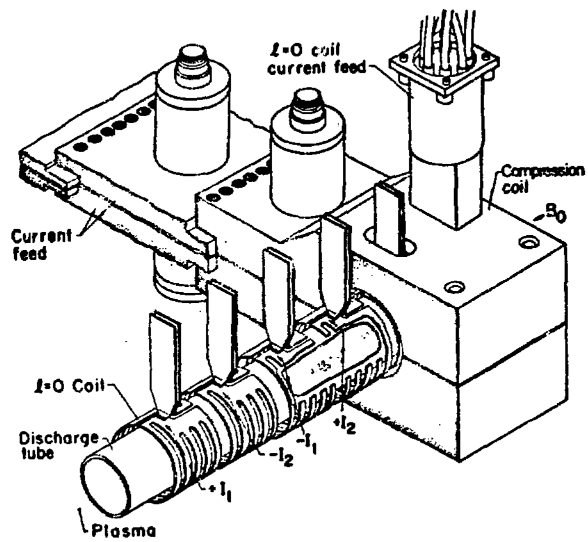

Fig. 8. Arrangement of the $\ell = 0$ feedback coils in the main Scyllac coil.

IV. WALL STABILIZATION AND STAGED THETA PINCHES

Adopting the assumption that the m = 1 motion is indeed the MHD instability predicted on the Princeton-NYU ordering [9,10], as indicated by Scylla IV-3 experiments [4], sharp-boundary theory gives the following dispersion relation:

$$\gamma^2 = h^2 v_A^2 \left[-\beta^2 \left(\frac{a}{b}\right)^4 \delta_1^2 + \frac{\beta(4-3\beta)(2-\beta)}{8(1-\beta)} h^2 a^2 \delta_1^2 + \frac{\beta(3-2\beta)(1-\beta)}{(2-\beta)} \delta_o^2 \right], \qquad (6)$$

where a/b is the ratio of plasma and coil wall radii. The first term is a wall stabilization term arising from the $\ell = 1$ dipole currents in the plasma, as illustrated in Fig. 9. This term appears in all the theories, including those with diffuse plasma profiles, regardless of which expansion is used. Freidberg has also derived the first term using a simple magnetostatic model [15] with line dipole currents. The second and third terms are the destabilizing terms arising from the $\ell = 1$ and $\ell = 0$ fields.

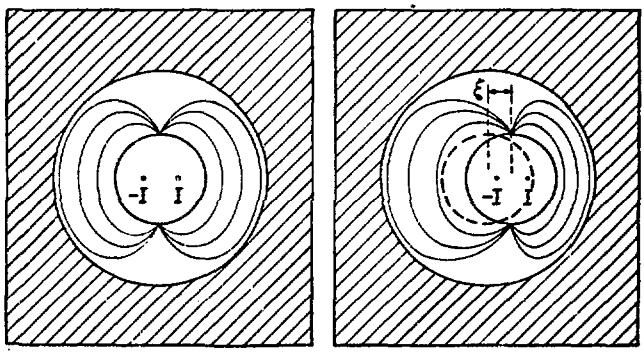

Fig. 9. Illustrating wall stabilization by $\ell = 1$ fields in θ-pinches.

From Eq. (6) it follows that the m = 1 mode can be stabilized by making the wall term dominate, that is by making ha and δ_o small. However, the requirement for toroidal equilibrium,

$$\delta_1 = -\frac{2}{3-2\beta} \frac{a}{R} \frac{1}{h^2 a^2 \delta_o} , \qquad (7)$$

must also be satisfied. It is not possible with present Scyllac values of a/b to make both ha and δ_o small, keeping $\delta_1 \sim 1$, without requiring unacceptably large aspect ratios R/a.

A second approach to make the wall term dominate is to make the ratio a/b larger. Conventional θ-pinches produce highly compressed plasmas with a/b ~ 0.1. Because of this the dominant m = 1 motion in Scyllac-type experiments must be feedback stabilized. Despite the fact that the m = 1 mode is predicted to be only weakly unstable for an $\ell = 1,0$ system, the technological requirements on the feedback system are quite demanding. As a result, it is important to make wall stabilization effective. By creating a plasma with $\beta \simeq 0.8$, $\delta_1 \simeq 1$, $\delta_o \simeq 0.1$ and a/b ~ 0.3 to 0.5 it should be possible to wall stabilize the m = 1 mode. This will first be accomplished in linear-staged θ-pinch experiments and later in toroidal experiments. The staging principle is illustrated in Fig. 10.

The staged θ-pinch uses fast-implosion heating and subsequent slow compression from separate energy sources. In this arrangement the implosion heating can be increased with less subsequent compression heating to produce increased a/b ratios to satisfy the wall stabilization requirements. The staged experiments at LASL will involve conventional filling densities and implosion-heating electric fields $\gtrsim$ 2 kV/cm at the inside of the tube, substantially larger than in the past. In the staged experiments the implosion-heated plasma will be further compressed using an 800-kJ, 50-kV capacitor bank, to demonstrate the staging process. The implosion-heating compression coil will have a length of 4.5-m, a coil bore of 22.4-cm, and a discharge tube bore of 20 cm. The compression field will be variable between 10 to 20 kG with a crowbarred e-folding time of approximately 50 μsec. The plasmas which will be produced in the staged θ-pinch will be collisionless with ion temperatures in the range 1.3 to 2.5 keV and compressed plasma densities in the range 0.2 to 0.8 x 10^{16} cm^{-3}. From Eq. (6), wall stabilization of the ℓ = 1 driven, m = 1 mode should occur provided the ratio of the plasma radius to coil radius has a value given by:

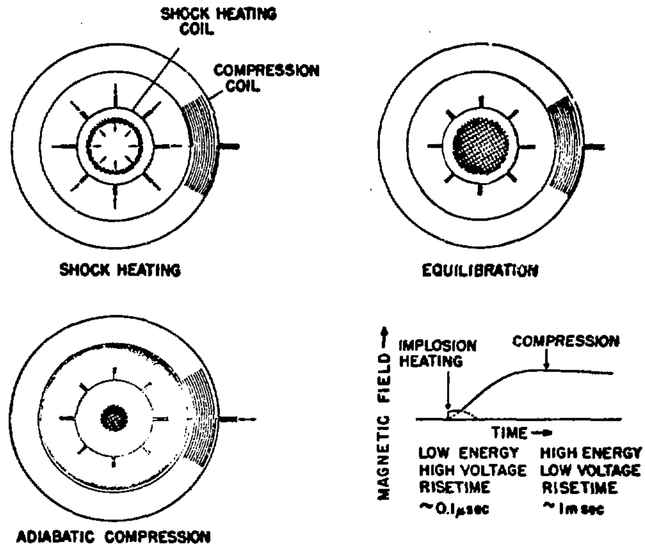

Fig. 10. Principles of the staged θ-pinch.

$$\left(\frac{a}{b}\right)^4 \geq \frac{(4-3\beta)(2-\beta)}{(1-\beta)} (ha)^2 \quad . \qquad (8)$$

For plasma parameters: a = 3 cm, δ_1 = 1.0, β = 0.8, and ha = 0.13, Eq. (8) gives a/b = 0.4. In the wall stabilization experiments on the linear 4.5-m θ pinch, an ℓ = 1 helical field will be superimposed on the axial field to drive an m = 1 instability. With the larger a/b ratios, wall stabilization of the mode can be studied in detail. The staged θ pinch is particularly suited for these experiments since the implosion and compression phases of the heating can be varied independently to produce various a/b ratios.

VI. EXPERIMENTS WITH THE 5-METER LINEAR SCYLLAC THETA PINCH

A. Experimental Arrangement.

The linear Scyllac experiment was a five-meter-long, straight theta pinch which used 5 of the 15 Scyllac capacitor racks to supply energy to the main compression coil. Two additional capacitor racks with a separate trigger system energized the 16-cm-long mirror coils. The inside diameter of both the main and mirror coils was 11 cm, and the quartz discharge tube had an inside diameter of 8.8 cm. The main bank was operated at 45 kV and the mirror bank at 40 and 45 kV. The magnetic field waveforms are shown in Fig. 11.

B. Results Without Magnetic Mirrors.

With an initial filling pressure of 10-mTorr D_2, the plasma had a measured density profile which was approximately Gaussian with an inflection-point radius of 0.8-1.0 cm, a peak density of $1.5\text{-}2.0 \times 10^{16}/cm^3$, and an ion temperature (as indicated by neutron yields) of 2.5-3 keV. The plasma column exhibited the previously observed [13,16] "wobble" which usually began 4 to 5 μsec after the initiation of the main discharge. The top frame of Fig. 12 shows streak camera photographs which illustrate the plasma wobble.

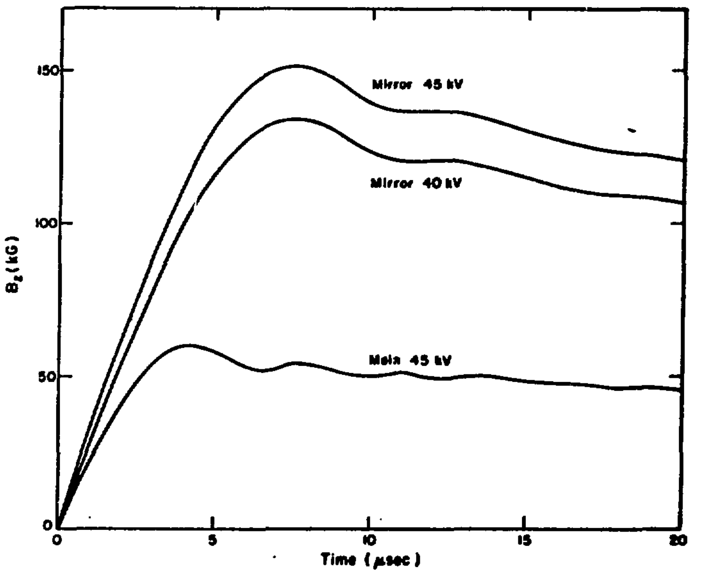

Fig. 11. B_z waveforms for main and mirror fields of the 5-m linear theta-pinch experiment.

The time for propagation of an Alfvén wave from the ends of the coil, using the peak magnetic field and the plasma density on axis, is about 4 μsec. The wobble is probably related to the shorting out of the electric fields in the plasma and the transfer of the diamagnetic current from the electrons to the ions [13,17]. The maximum amplitude of the wobble was about 1.5 cm from the discharge tube axis and the average value 0.5 to 1.0 cm. Stereoscopic views of the plasma column showed that the wobble was an m = 1 rotation with a frequency of about 300 kHz and an amplitude and phase which sometime varied along the coil axis.

C. Stability With Applied Mirror Fields.

The experiment was operated with mirror fields applied 0, 0.2, 0.5, and 1.0 μsec after the main compression field. The addition of the mirror field produced an m = 1,k ≈ 0 instability. (See the center frame of Fig. 12). For the zero delay and 0.2 μsec-delay cases this instability caused the plasma column to strike the discharge tube wall 5 to 8 μsec after initiation of the plasma discharge. For the larger delays (0.5 and 1.0 μsec) the movement of the plasma column was less, the plasma column never striking the discharge tube wall before 15 μsec and sometimes (particularly, with the mirror bank operated at 40 kV) the plasma column never struck the wall (bottom frame of Fig. 12). A change in the discharge tube geometry which shortened the distance between the plasma column and the discharge tube (measured along magnetic field lines) increased the stability of the plasma column. This indicates that the difference in plasma behavior with different mirror field delays is due to line-tying effects. With delayed application of the mirror fields, line-tying has a chance to become effective before the mirror ratio becomes large.

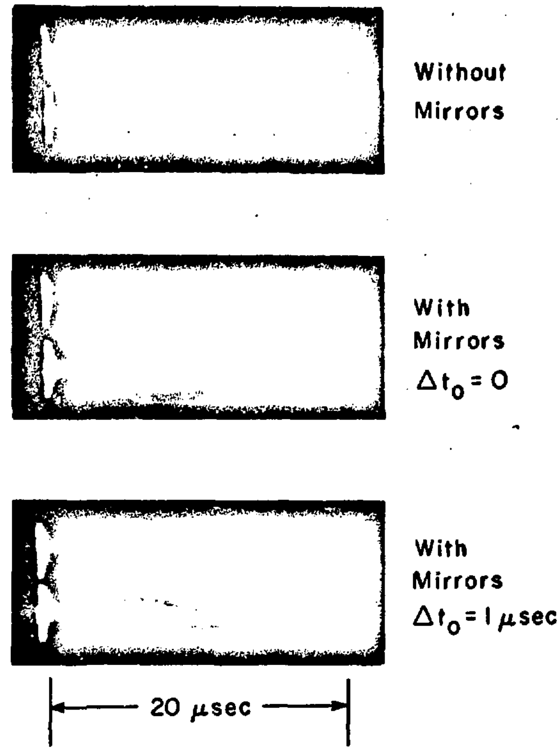

Fig. 12. Streak photographs from the 5-m linear theta pinch showing a no-mirror case and two mirror cases.

D. Plasma Confinement.

Plasma loss out the ends of the theta-pinch was measured using end-on holographic interferograms [13] for the case of no applied mirror field and for the case of delayed application (1.0 μsec) of the mirror field and mirror bank operation at 40 kV. Results are shown in Fig. 13. The end-loss time with applied mirror fields is 18.9 μsec, while that without mirrors is 11.5 μsec. These loss rates were compared with two theoretical models, a computer simulation by W. P. Gula [18] and an analytical model by J. P. Freidberg which extended the model of Morse [19] to diffuse plasma profiles. The two theoretical models are in agreement and predict a loss rate of 16-18 μsec without mirror fields and an increase of plasma confinement by about the mirror ratio (2.5) when mirror fields are added. The predicted loss rates, as well as their ratio, are in considerable disagreement with the experimental results. The experimental end loss times, however, scale from previous experimental results on Scylla IV-1 [20] and Scylla IV-3 [13] if it is assumed that the loss time varies as $L/T_i^{1/2}$ where L is the length of the coil and T_i is the ion temperature. Table I compares observed end loss times

TABLE I

END LOSS SCALING IN THETA PINCHES

	Length (m)	T_i (keV)	n (10^{16} cm^{-3})	τ observed (μsec)	τ scaled (μsec)
Scylla IV-1	1	3.2	2.1	2.4	2.13
Scylla IV-3	3	1.4	3.2	10.1	9.67
Scyllac Linear	5	2.7	2.0	11.5	11.50

in the three experiments without mirrors to the predicted values, normalized to the linear Scyllac data point.

E. Plasma Electron Temperature.

The electron temperature was measured by 90° Thomson scattering at 6943Å. The electron temperature at peak field was 610 ± 110 eV. The experimental value at peak field agrees well with the value (∿600 eV) predicted by the theoretical model of Morse [19] in which the electron temperature is determined by the relative rates at which energy is supplied to the electrons by collisions with the ions and is in turn lost out the ends of the main coil by electron thermal conduction. The theory correctly predicted the observed electron temperature for Scylla IV-1 [20], Scylla IV-3 [21], and the Scyllac linear experiment as shown in Table II.

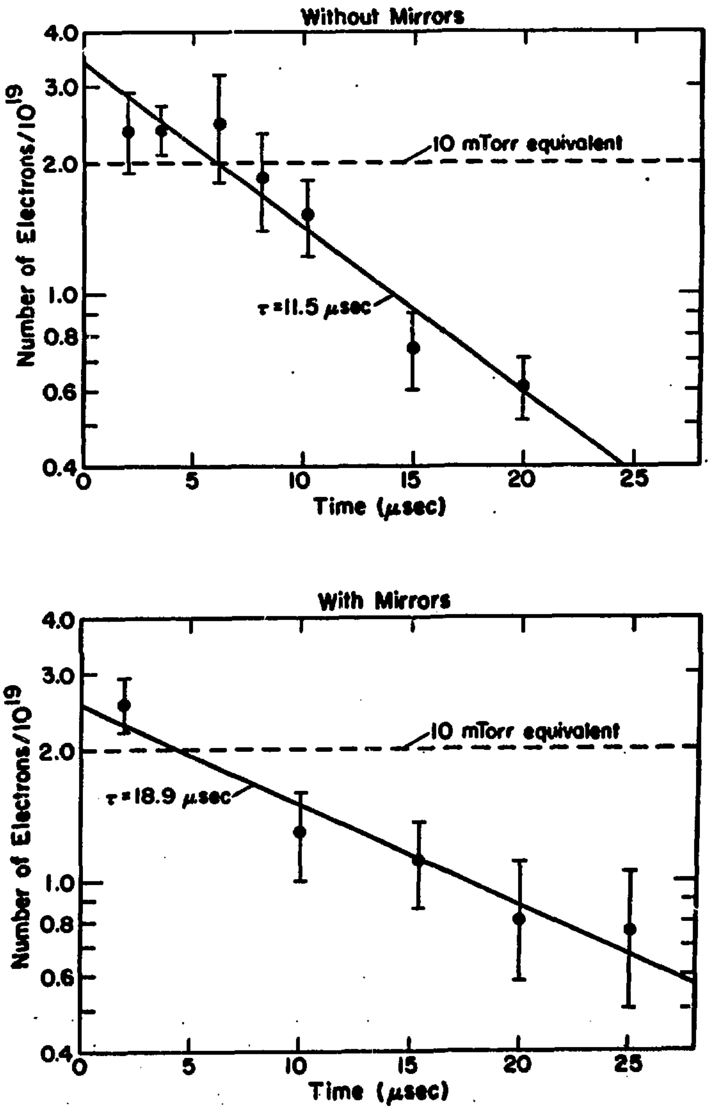

Fig. 13. End loss in the 5-m linear experiment with and without magnetic mirrors.

TABLE II

ELECTRON TEMPERATURE SCALING WITH PLASMA LENGTH

	Length (m)	T_e observed (keV)	T_e predicted (keV)
Scylla IV-1	1	.33	.29
Scylla IV-3	3	.39	.43
Scyllac Linear	5	.61	.53

REFERENCES

1. W. R. Ellis, et. al., Proc. 2nd Topical Conf. Pulsed High-Beta Plasmas, Max-Planck-Institut fur Plasmaphysik Report IPP 1/127, July 1972.
2. F. C. Jahoda, et. al., Proc. Fifth European Conference on Controlled Fusion & Plasma Physics, Grenoble, Aug. 1972.
3. K. S. Thomas, et. al., Proc. 2nd Topical Conference Pulsed High-Beta Plasmas, Max-Planck-Institut fur Plasmaphysik, Report IPP 1/127, July 1972.
4. K. S. Thomas, et. al., Phys. Fluids 15, 1658 (1972).
5. R. F. Gribble, et. al., Proc. 2nd Topical Conference Pulsed High-Beta Plasmas, Max-Planck-Institut fur Plasmaphysik, Report IPP 1/127, July 1972.
6. F. L. Ribe & M. N. Rosenbluth, Phys. Fluids 13, 2572 (1970).
7. H. Weitzner, Phys. Fluids 14, 658 (1971).
8. J. P. Freidberg, Plasma Phys. Contr. Nucl. Fusion Res. 3, 215 (1971).
9. M. N. Rosenbluth, et. al., Phys. Fluids 12, 726 (1969).
10. H. Grad & H. Weitzner, Phys. Fluids 12, 1725 (1969).
11. J. P. Freidberg & B. M. Marder, Phys. Fluids 14, 174 (1971).
12. F. L. Ribe, et. al., "Proposed Experiments on Heating, Staging, and Stabilization of Theta Pinches", Los Alamos Scientific Laboratory Report LA-5026-P.
13. R. F. Gribble, W. E. Quinn, & R. E. Siemon, Phys. Fluids 14, 2042 (1971).
14. K. I. Thomassen, Los Alamos Scientific Laboratory Report LA-4598-MS, 1971.
15. J. P. Freidberg, Phys. Fluids, to be published.
16. H. A. B. Bodin, et. al., Plasma Phys. Contr. Nucl. Fusion Res. 1, 193 (1971).
17. K. S. Thomas, Phys. Rev. Letters 23, 746 (1969).
18. W. P. Gula, to be published.
19. R. L. Morse, Phys. Fluids, 11, 1558 (1968).
20. E. Little, W. Quinn, & G. Sawyer, Phys. Fluids 8, 1168 (1965).
21. K. S. Thomas, et. al., Phys. Fluids 15, 1658 (1972).

*Work performed under the auspices of the United States Atomic Energy Commission.